

Preparatory Attention Relies on Dynamic Interactions between Prelimbic Cortex and Anterior Cingulate Cortex

Nelson K. B. Totah^{1,2,3}, Mark E. Jackson^{3,4} and Bita Moghaddam^{1,3}

¹Center for Neuroscience at the University of Pittsburgh, ²Center for the Neural Basis of Cognition and ³Department of Neuroscience, University of Pittsburgh, Pittsburgh, PA 15260, USA and ⁴Department of Biology, Central Connecticut State University, New Britain, CT 06050, USA

Address correspondence to Dr Bita Moghaddam, A210 Langley Hall, Pittsburgh, PA 15260, USA. Email: bita@pitt.edu.

An emerging view of prefrontal cortex (PFC) function is that multiple PFC areas process information in parallel, rather than as distinct modules. Two key functions assigned to the PFC are the regulation of top-down attention and stimulus-guided action. Electrophysiology and lesion studies indicate the involvement of both the anterior cingulate cortex (ACC) and prelimbic cortex (PL) in these functions. Little is known, however, about how these cortical regions interact. We recorded single unit spiking and local field potentials (LFPs) simultaneously in rodents during a sustained attention task and assessed interactions between the ACC and PL by measuring spike-LFP phase synchrony and LFP-LFP phase synchrony between these areas. We demonstrate that the magnitude of synchrony between the ACC and PL, before stimulus onset, predicts the subjects' behavioral choice after the stimulus. Furthermore, neurons switched from a state of beta synchrony during attention to a state of delta synchrony before the instrumental action. Our results indicate that multiple PFC areas interact during attention and that the same neurons may participate in segregated assemblies that support both attention and action.

Keywords: ADHD, functional connectivity, schizophrenia, phase synchrony, preparatory attention

Introduction

It is widely accepted that a top-down attention signal originates from the prefrontal cortex (PFC) (Posner and Petersen 1990; Desimone and Duncan 1995; Fuster 2001; Miller and Cohen 2001; Roelofs et al. 2006; Eigner et al. 2008; Gregoriou et al. 2009; Orr and Weissman 2009). Previous studies have implicated various PFC modules, such as the anterior cingulate cortex (ACC), the frontal eye fields, and the dorsolateral PFC (dlPFC) as being responsible for priming the representation of an expected stimulus in sensory cortex (Johnston et al. 2007; Totah et al. 2009; Noudoost et al. 2010). An emerging view of PFC function is that discrete areas process information in a coordinated manner rather than as distinct modules (Duncan 2001; Moghaddam and Homayoun 2007). Coordinated activity between neurons in different networks and brain regions may be mediated by spike synchrony with local field potential (LFP) oscillations (Varela et al. 2001; Fries 2005) as well as synchrony of LFP oscillations, which provide windows of time when the effectiveness of a proximal spike on a distal neuron's post-synaptic potential is enhanced (Buzsáki and Draguhn 2004; Womelsdorf et al. 2007; Canolty et al. 2010). Although the effects of engaging top-down attention on synchrony between visual cortex areas have been studied (von Stein et al. 2000; Fries et al. 2008), less is known about synchrony-mediated communication between PFC areas during top-down attention.

In order to study the interactions between PFC areas during top-down attention, we recorded single unit spiking and LFP from 2 rat PFC areas during a rodent attention task and measured phase synchrony between brain regions. The regions included the ACC and the prelimbic cortex (PL), both of which have been implicated in attention and stimulus-guided action (Passetti et al. 2002; Chudasama et al. 2003; Peters et al. 2005; Narayanan and Laubach 2006, 2009; Ng et al. 2007). In the task, rats were trained to anticipate a brief visual stimulus, which appeared at 1 of 3 randomly selected locations, and to make an instrumental response to the perceived location. We focused the analysis on phase synchrony between the 2 PFC areas before stimulus onset (i.e., during top-down attention) and before the instrumental response (i.e., before the stimulus-guided response). Prior to the onset of a behaviorally relevant stimulus, preparatory attention improves selection of an expected stimulus by enhancing the firing rate of sensory cortex neurons that will represent the stimulus (Chelazzi et al. 1993; Luck et al. 1997; Chawla et al. 1999, 2000; Driver and Frith 2000; Bressler et al. 2008; Stokes et al. 2009; Sylvester et al. 2009). Accordingly, we focused our analysis of preparatory attention on the prestimulus period, when the rat orients to and waits for the upcoming stimulus. The analyses compared correct trials with incorrect trials, when the rat responded to one of the nonilluminated stimulus locations. We interpreted incorrect trials as being indicative of a preparatory attention signal that is inadequate for selecting the correct stimulus location. While we cannot eliminate the possibility that incorrect selection of stimulus location is due to deficient planning or stimulus expectation, these cognitive abilities are related in that they rely on PFC neural activity before onset of a behaviorally relevant stimulus and have similar effects on sensory cortex neural activity (Niki and Watanabe 1979; Pragay et al. 1987; Fuster 1995; Luck et al. 1997; Kastner et al. 1999; Rainer et al. 1999; Driver and Frith 2000; Ghose and Maunsell 2002; LaBerge 2002; Johnston et al. 2007; Hussar and Pasternak 2009; Stokes et al. 2009; Sylvester et al. 2009; Totah et al. 2009). In addition to studying preparatory attention, we assessed synchrony between the ACC and PL before the stimulus-guided instrumental response in order to characterize how these PFC areas interact during action preparation and execution. We hypothesized that, if multiple PFC areas need to coordinate their activity to generate preparatory attention and stimulus-guided behavior, then synchrony would predict performance accuracy.

Materials and Methods

Animals

Four male Sprague-Dawley rats were used in this study. All rats were housed on a reverse light cycle and trained and tested during the rats'

active phase. All experiments were carried out in compliance with the University of Pittsburgh Institutional Animal Care and Use Committee (IACUC).

Behavioral Task

The behavioral task has been described previously (Totah et al. 2009). Briefly, rats were trained and tested in operant chambers with a house light on the ceiling, 3 stimulus ports with internal light-emitting diodes on one wall and an illuminated food magazine on the wall opposite from the stimulus ports. Nose pokes into the stimulus ports and the food magazine were registered by photosensors. A correct response, consisting of a nose poke into an illuminated stimulus port, was rewarded with sucrose. An incorrect response into an unlit stimulus port resulted in an extinguished house light. The rat was required to nose poke into a stimulus port within 5 s after stimulus onset; otherwise, the house light was extinguished (i.e., an omission trial). The rat initiated each trial with a poke into the food magazine, which contained either sucrose pellets or was empty depending on whether the previous trial was correct or an error (i.e., an incorrect or omission trial).

At the start of a trial, an 8-s prestimulus period passed before the stimulus onset. On each trial, one of the 3 stimulus ports would illuminate. The location of the stimulus was selected at random from the 3 stimulus ports. There was a balanced distribution of the selection of the 3 ports, but the order of presentation was random. Rats initially were trained to respond to a 15-s duration stimulus and could respond during the stimulus or within 5 s after the stimulus was extinguished. Each session lasted 30 min. Based on satisfying performance criteria (for detailed information regarding training, see previous work by Totah et al. 2009), the stimulus duration was gradually reduced to 300 ms. Rats were deemed ready for electrode implantation when they met the performance criterion of >70% accuracy (i.e., number of correct responses/(number of correct responses + number of incorrect responses)) and <20% omissions (i.e., number of omitted responses/number of total trials) for 6 consecutive sessions using the 300 ms cue duration. The mean number of sessions needed to complete training was 42 sessions. Rats exhibited attentive behavior, whereby they oriented to the operant chamber wall that contained the stimulus ports and waited for the stimulus. Orientation to the wall of stimulus ports began approximately 2 s before stimulus onset and was maintained throughout the prestimulus period. It was extremely rare (ca., <1% of trials across many 30-min sessions) for rats to orient away from the stimulus ports once they had begun orienting. Sessions were videotaped and reviewed in order to eliminate trials in which the rat did not directly face the stimulus ports because those were not stereotypical task behaviors.

Electrophysiology Procedure

Rats were implanted under isoflurane anesthesia with 2 microelectrode arrays each consisting of 8 Teflon-insulated stainless steel wires in a 2 × 4 pattern measuring 0.25 mm × 0.70 mm with an impedance of 300–700 kΩ (NB Labs, Denison, TX). One array was placed spanning the ACC: -0.2 to -1.0 mm posterior to bregma, -0.4 to -0.7 mm lateral to bregma, and -2.5 mm ventral from the dura surface and one array was placed spanning the contralateral PL: +2.4 to +3.4 mm anterior to bregma, +0.5 to +0.8 mm lateral to bregma, and -3.8 mm ventral from the dura surface.

After 1 week of recovery, rats were acclimated to attachment of the electrode cable in the operant box for four 30-min sessions and retrained to criterion performance at the 300 ms stimulus duration. Once behavioral performance was stable and above criterion, a 30-min session was recorded. Single units and LFP were recorded via a unity-gain field-effect transistor headstage and lightweight cabling, which passed through a commutator to allow freedom of movement. Neural activity was amplified using a 1000× gain, and single unit activity was band pass filtered at 300–8000 Hz and LFP was band pass filtered at 0.7–170 Hz. Neural activity was digitized at a rate of 40 kHz and LFPs were down sampled to 1 kHz using Recorder software (Plexon, Inc.). Single-unit activity was digitally high-pass filtered at 300 Hz and LFP was digitally low-pass filtered at 125 Hz. Signals from the operant box were

used as event markers to coordinate behavioral events with neural activity. Units were isolated in Off-Line Sorter software (Plexon, Inc.). Stability of units over time was confirmed by viewing the waveform clusters in a 3D space of the first 2 principal components and time. Units were rejected if the interspike interval histogram was inconsistent with a refractory period of <1.1 ms.

Data Analysis

Electrophysiological data were analyzed with custom scripts written in Matlab (Mathworks, Natick, MA). An LFP signal was collected from one electrode in each brain region. The signal was aligned to the behavioral event of interest and trials with LFP clipping in either brain region were removed from analysis. The LFP signal was convolved with a complex Morlet wavelet, resulting in a complex number, $W(f,t)$, at each scale (converted to a frequency for simplicity), f , and time, t . The conversion from scale to frequency resulted in all plots of frequency space appearing nonuniform because wavelet transformation results in higher resolution at lower frequency. Power spectra were calculated as $|W(f,t)|^2$ for each time-frequency bin on each trial. Each time-frequency bin was normalized to percentage maximum power on a trial-by-trial basis. Normalized power spectra then were averaged across trials. The presented spectrograms are the average across all 4 animals.

Phase synchrony between LFP signals was measured as a phase locking value (PLV) over time in each trial and averaged across trials within animals. The constancy of the difference in phase between the LFP signals at electrodes, j and k , was calculated as a PLV, such that

$$PLV_{j,k}(f, t) = \frac{1}{N} \left| \sum_N e^{i(\phi_j - \phi_k)} \right|,$$

where N is the number of samples in the time window, ϕ is phase, and $| |$ is the complex modulus (Lachaux et al. 1999; Rodriguez et al. 1999). PLV ranges from 0 to 1 (constant phase difference). The PLV is equivalent to 1 minus the circular variance of the phase differences. Phase angle was extracted from $W(f,t)$ using

$$\theta(f, t) = \tan^{-1} \frac{\Im\{W(f, t)\}}{\Re\{W(f, t)\}},$$

where $\theta(f, t)$ is phase angle at a time and frequency point and \Im and \Re are the imaginary and real components of the wavelet coefficient, respectively. For each frequency of interest, PLV was calculated using a time window consisting of 10 cycles and slid in steps of one-twentieth of a time window. Because synchrony between 2 oscillatory signals can occur by chance, we used a surrogate data set to determine if the occurrence of synchrony was greater than expected by chance. We computed a distribution of PLVs that would be expected if the 2 LFP signals were independent of one another by computing 200 surrogate PLV values with a random trial selected for one of the electrodes (see above references). If the observed PLV was higher than the upper limit of the 95% confidence interval of the distribution of surrogate PLV values, then the PLV was not spurious.

Spike-LFP phase synchrony was calculated in 2-s time windows slid in 200-ms steps (prestimulus period) and in 1-s time windows slid in 100-ms steps (instrumental nose poke period). To assess the phase locking characteristics of a neuron, we collected the LFP phase angles that corresponded to the spike times for all spikes within a time window, across all trials (Fig. 1). A neuron was considered significantly phase locked if the distribution of spike phase angles departed from a uniform circular distribution (Rayleigh's test for circular uniformity, $P < 0.05$). The circular statistics toolbox (MATLAB) was used for statistical analyses of spike-LFP phase synchrony (Berens 2009). If any time window had <6 spikes, we could not rely on Rayleigh's test (Fisher 1996), and we chose to remove that neuron from analysis. The value of Rayleigh's Z statistic for a neuron was used as a measure of phase consistency or the strength of spike-LFP phase locking. Rayleigh's Z was calculated by

$$Z = nR^2,$$

where R is the mean resultant phase vector length of n spikes. The P value for Rayleigh's test for circular uniformity is calculated as:

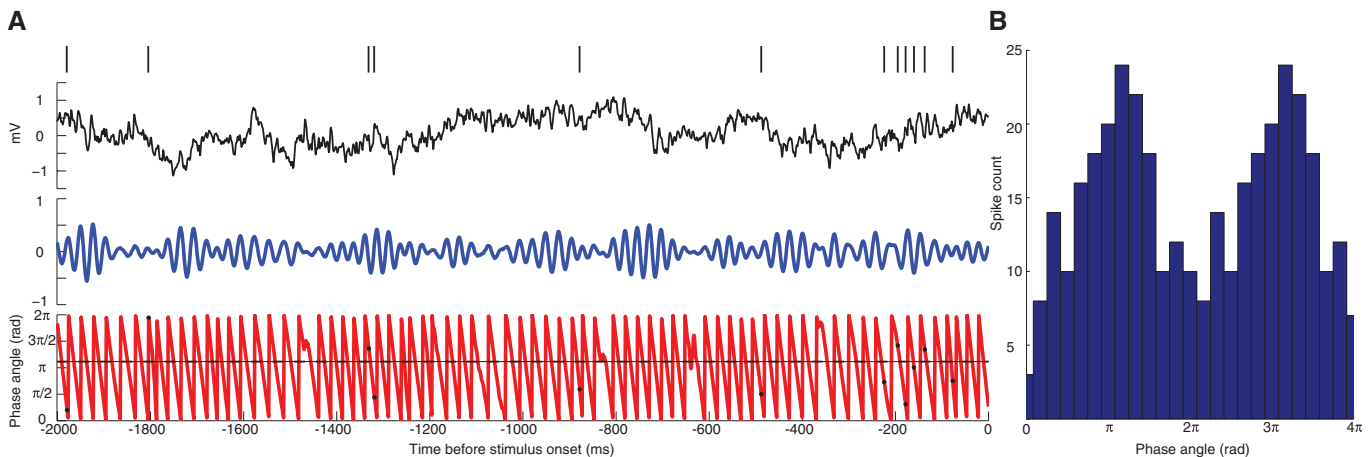


Figure 1. Summary of the method of analysis of spike-LFP phase locking. Spike times (*A*, top) and LFP (*A*, black) were recorded simultaneously. (*A*) Data are plotted for a single example trial during the 2 s before stimulus onset ($t = 0$). The LFP was convolved with a complex Morlet wavelet. The amplitude (blue) and phase angle (red) at 40 Hz are plotted below the raw data. Spike times are indicated by black dots on the plot of phase angle (red). In this trial, the spikes tend to occur around the mean resultant angle (dotted black line), which was calculated using spike times from all trials for this neuron. (*B*) Spikes from the 2 s before stimulus onset combined across all trials, for the same neuron as in (*A*). The neuron was significantly phase locked (Rayleigh's test for circular uniformity, $Z = 8.936$, $P < 0.0001$) and the mean phase angle was 3.504 radians.

$$P = e^{-Z} \times \left(1 + \frac{2Z - Z^2}{4n} - \frac{24Z - 132Z^2 + 76Z^3 - 9Z^4}{228n^2} \right).$$

Neurons were considered significantly phase locked if $P < 0.05$. We controlled for spurious spike-LFP phase locking, while keeping the timing of behavioral events intact, by computing spike-LFP phase locking between spikes from a trial and the LFP signal from a different, randomly selected trial (without replacement). A distribution of the expected spurious phase locking was formed by calculating Rayleigh's Z values on 200 sets of trial shuffled data. For each time-frequency bin, the upper limit of the 95% confidence interval of the distribution was selected as the expected spurious Rayleigh's Z for that particular neuron in that particular time-frequency bin. Rayleigh's Z values were compared between the original data (correct trials) and the shuffled data using a 2-way repeated measures analysis of variance (ANOVA) (with factors data type and time).

We were particularly interested in comparing the phase locking of neurons on correct and incorrect trials; however, there are fewer incorrect trials and, accordingly, a smaller sample size of spikes with which to calculate R . To equalize any bias due to unequal sample sizes, we employed a resampling procedure. For a given neuron with x number of spike times in the correct condition and y number of spike times in the incorrect condition (where $x > y$), we removed y number of spikes (selected randomly without replacement) from the correct condition and replaced them with all of the y number of spikes from the incorrect condition. We calculated Rayleigh's Z for the new group with replaced spike times. We repeated this resampling procedure 5000 times and calculated Rayleigh's Z on each iteration. We then used the mean of the Z distribution to calculate a P value for that neuron. Thus, the same number of spikes per neuron is present in both correct and incorrect conditions. Accordingly, conditions labeled as "incorrect" in the spike-LFP phase locking analysis reflect the degree to which the insertion of the spike times from incorrect trials degrades or enhances spike-LFP phase locking observed on correct trials. This is similar to the method employed by Siegel et al. (2009) to control for the same sample size bias (Siegel et al. 2009). We also tried a bootstrapping procedure to control for the sample size bias, whereby we randomly subsampled y random spikes (with replacement) from the full sample in the correct condition (5000 iterations). However, we found that this reduced the power of the Rayleigh's Z test for neurons with a large sample of spikes, which is in line with the findings of others (see Supplementary Materials, Sirota et al. 2008).

Histology

At the completion of recordings, rats were anesthetized with chloral hydrate, and the rats were perfused with normal saline for 10 min and

10% buffered formalin for 10 min. After fixation, brains were sectioned and stained using cresyl violet. Placement of electrode tips was confirmed under a light microscope and subjects' neural activity recorded from improperly placed electrodes was excluded from analysis.

Results

Broadband LFP Oscillations Occur before the Stimulus and Are Related to the Subsequent Behavioral Choice

Across all rats, there were 38 ± 4 correct choice trials and 13 ± 3 incorrect choice trials (after removal of trials with LFP artifacts). Figure 2 shows mean power spectrograms averaged across all animals. We examined the 2-s window before stimulus onset, which corresponds to the approximate time of orientation to the wall of stimulus ports (Totah et al. 2009). We found that power was reduced on incorrect trials across a range of frequencies (*t*-test for each time-frequency bin, Fig. 2, right panel). Additionally, the alpha power had a typical "waxing and waning" rhythm that has been observed previously (Linkenkaer-Hansen et al. 2001, 2004). The remaining analyses were focused on studying phase synchrony and excluded LFP amplitude from the analysis (Lachaux et al. 1999; Varela et al. 2001; Le Van Quyen and Bragin 2007).

Prestimulus Within-Region Phase Locking Predicts the Behavioral Choice after Stimulus Onset

We recorded 32 neurons in the ACC and 61 neurons in the PL. During the 2-s period preceding the stimulus onset, neurons in both PFC areas were phase locked across a wide range of frequencies (Rayleigh's test for circular uniformity, $P < 0.05$). Compared with incorrect trials, a larger proportion of neurons phase locked to various frequencies (between 1.5 and 50.0 Hz) on correct trials (Table 1). At many frequencies, a similar proportion of neurons were phase locked on correct and incorrect trials (Fig. 3). In the ACC, Within-region delta band phase locking was reduced during incorrect trials ($\chi^2 = 4.27$, $P < 0.05$; Fig. 3*A*), whereas in the PL, Within-region beta band phase locking was reduced during incorrect trials ($\chi^2 = 4.14$, $P < 0.05$, Fig. 3*B*). The reduced proportion of phase locked

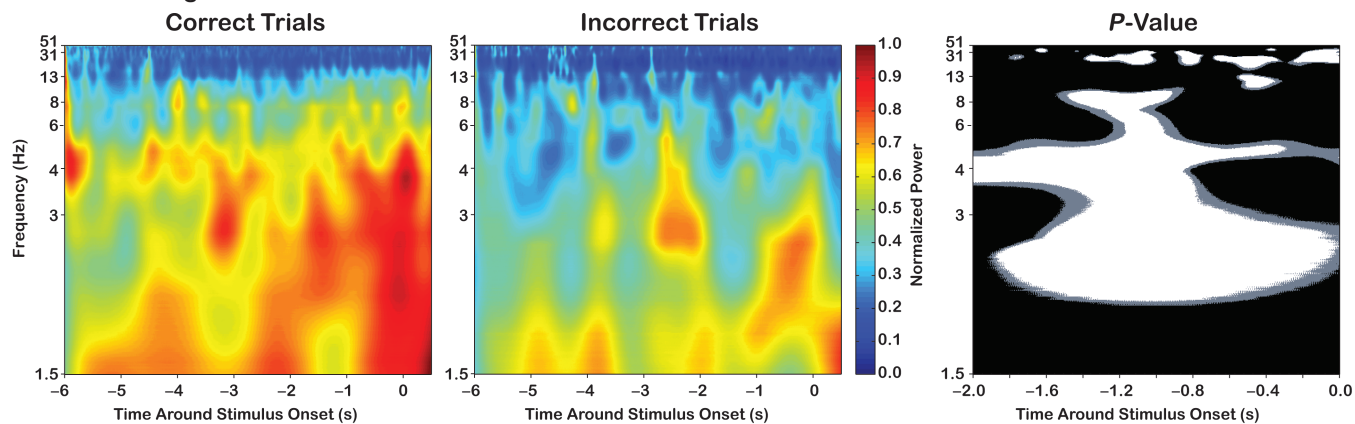
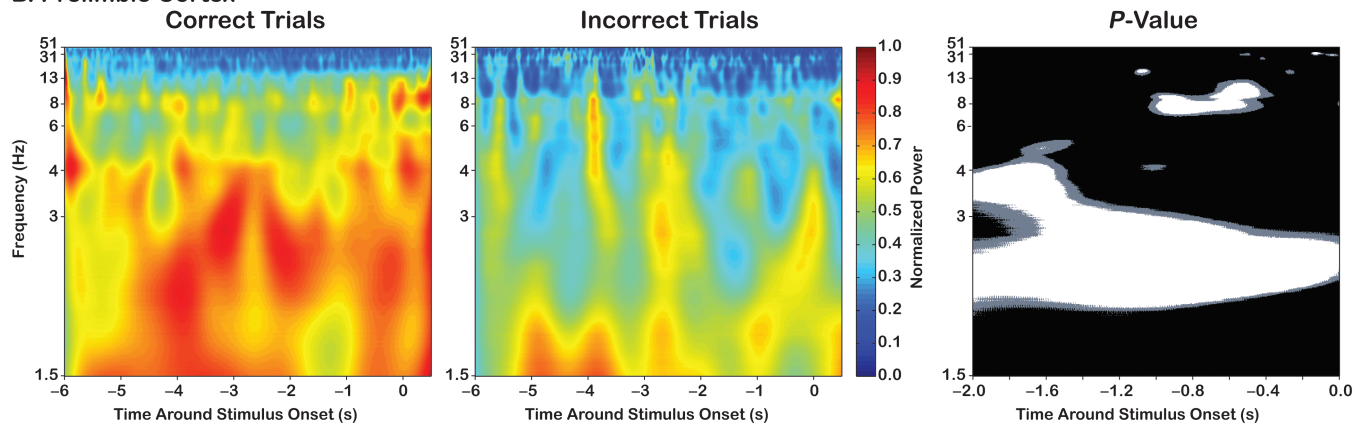
A. Anterior Cingulate**B. Prelimbic Cortex**

Figure 2. Prestimulus broadband LFP power is correlated with trial type. The spectrogram shows the mean normalized LFP power averaged across 4 rats. Stimulus onset is at $t = 0$ s. Power was normalized within trial and then averaged across trials, within subject. Data are shown for correct trials (left) and incorrect trials (middle) for both the ACC (A) and PL (B). A t -test was used to compare each time-frequency bin between trial types. The results are plotted (right) using black if P was not significant, gray if $0.05 \leq P < 0.08$, and white if $P < 0.05$. In both brain regions, delta (1–4 Hz), alpha (8–12 Hz), and beta (13–30 Hz) powers are greater on correct trials. However, the time course and frequency spread is not the same in both brain regions. Although not different between trial types, the power of alpha oscillations fluctuated over time in a periodic manner.

Table 1

The number and percent of neurons that were phase locked to any frequency between 1.5 and 51.0 Hz during -2 to 0 s before stimulus onset

	Within region		Between region	
	ACC ($n = 32$)	PFC ($n = 61$)	ACC spikes PL LFP ($n = 32$)	PL spikes ACC LFP ($n = 61$)
Correct trials, prestimulus	25 (78%)	41 (67%)	24 (75%)*	40 (66%)**
Incorrect trials, prestimulus	21 (66%)	36 (59%)	17 (53%)	28 (46%)

Note: During incorrect trials, a larger proportion of neurons did not phase lock to LFP oscillations. In the case of cross-regional phase locking, the effect reached a trend (ACC spikes/PL LFP) and significance (PL spikes/ACC LFP). * $P < 0.07$ (chi-squared test for independence), ** $P < 0.05$.

neurons was centered at 1.6 Hz in the delta band (ACC) and 17 Hz in the beta band (PL).

To study how phase locking strength varied over the prestimulus time period, we compared time-resolved Rayleigh's Z for ACC neurons that were phase locked at 1.6 Hz and PL neurons that were phase locked at 17 Hz during the 2-s window before stimulus onset. The mean, time-resolved Rayleigh's Z across delta band phase locked ACC neurons was reduced on incorrect trials (Fig. 3C) (ANOVA; main effect of trial: $F_{1,3} = 21.88$, $P = 0.019$; main effect of time: $F_{30,90} = 3.32$, $P < 0.001$; interaction: $F_{30,90} = 1.32$, $P = 0.158$). Comparing individual time points during the prestimulus period show that the difference between trial types is during the final 2-s

window before stimulus onset (post hoc t -test; $t_0 = 3.91$, $P = 0.008$). Although Rayleigh's Z in the theta band in the window ranging from -6 to approximately -3.5 s before stimulus onset appeared to be of higher magnitude on correct trials, this increase was not significant over time (ANOVA; interaction: $F_{30,90} = 0.725$, $P = 0.757$). Furthermore, phase locked neurons did not exhibit changes in firing rate nor did they differ between trial types (ANOVA; main effect of trial: $F_{1,3} = 8.51$, $P = 0.062$; main effect of time: $F_{39,117} = 0.89$, $P = 0.671$; interaction: $F_{39,117} = 1.194$, $P = 0.233$).

There was a trend for the mean, time-resolved Rayleigh's Z across beta band phase locked PL neurons to be reduced on incorrect trials (Fig. 3D) (ANOVA; main effect of trial: $F_{1,6} = 4.22$,

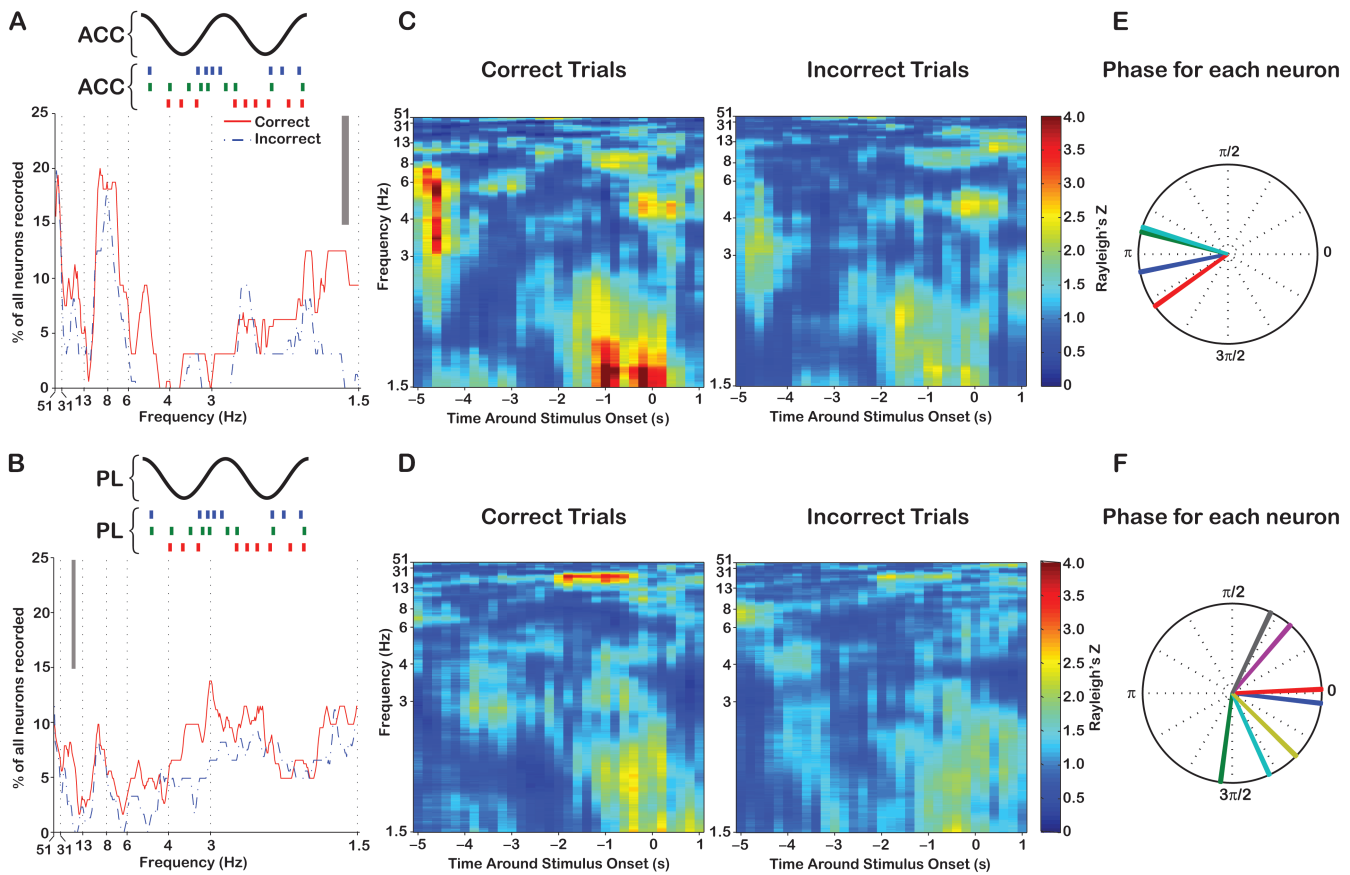


Figure 3. Within-region phase locking during the prestimulus period. (A) A schematic illustrating that the top panel (A,C,E) are data using ACC spikes and ACC field potentials. The proportion of neurons that were significantly (Rayleigh's test, $P < 0.05$) phase locked to frequencies between 1.5 and 50.0 Hz, during -2 to 0 s before stimulus onset, on correct (red, solid) and incorrect (blue, dotted) trials. The width of the vertical bar indicates frequencies at which there was a reduction in the proportion of phase locked neurons on incorrect trials (Chi-squared test, $P < 0.05$). (C) Mean, time-resolved, phase locking strength (Rayleigh's Z) is averaged across ACC neurons that phase locked to ACC delta (1–4 Hz) oscillations before stimulus onset. Stimulus onset is at $t = 0$ s. Rayleigh's Z was calculated in 2-s windows that were slid in 200 ms steps. Delta phase locking was reduced during incorrect trials. (E) The median phase angle of each ACC neuron illustrates that neurons are all phase locked to the trough of ACC delta oscillations (circular analog of Kruskal-Wallis test, $P =$ not significant indicating no difference in phase angle distribution between neurons). (B,D,F) Same as above. (B) A schematic illustrating that the bottom panel is data using PL spikes and PL LFP. A larger proportion of neurons phase locked to beta (13–30 Hz) oscillations on correct trials. (D) These neurons phase locked to beta oscillations during the prestimulus period on correct trials and phase locking strength was reduced on incorrect trials. (F) The PL neurons phase locked to the peak of PL beta oscillations.

$P = 0.086$; main effect of time: $F_{30,180} = 1.988$, $P = 0.003$; interaction: $F_{30,180} = 1.30$, $P = 0.151$). The difference between trial types occurred during the 2-s window before stimulus onset (post hoc t -test; $t_{12} = 3.99$, $P = 0.002$). Phase locked neurons did not modulate their firing rate over time, nor did they have a difference in firing rate between trial types (ANOVA; main effect of trial: interaction: $F_{39,234} = 0.889$, $P = 0.660$). Therefore, Within-region delta (within ACC) and beta frequency (within PL) phase locking strength before the stimulus predicted the animals' correct or incorrect choice after stimulus onset. Critically, the higher magnitude phase locking on correct trials was not spurious because it was eliminated when the trials were randomly shuffled (Within-region ACC ANOVA interaction: $F_{30,90} = 2.13$, $P = 0.002$; Within-region PL ANOVA interaction: $F_{30,180} = 2.59$, $P < 0.001$).

The preferred phase was measured for each neuron to determine whether neurons that were phase locked to local oscillations might spike with similar timing on correct trials. We calculated the median angle of the resultant vector and tested for a significant difference in spike phase angle distributions between phase locked neurons using a circular analog of the Kruskal-Wallis test. For the 4 neurons that were

phase locked to delta oscillations in the ACC (Fig. 3E), we found they shared a statistically similar phase angle of 3.2 rad ($P = 0.29$). In the PL (Fig. 3F), the 7 neurons that were phase locked to PL beta oscillations also shared a statistically similar phase angle of 4.9 rad ($P = 0.23$). Therefore, across animals and neurons, ACC neurons that phase locked to ACC delta oscillations preferred the trough of delta oscillations, whereas PL neurons phase locked to the peak of PL beta oscillations.

Prestimulus Between-Region Phase Locking Predicts the Behavioral Choice after Stimulus Onset

As a measure of communication across PFC areas, we measured Between-region spike-LFP phase locking. This analysis correlated spike times from the ACC with LFP phase recorded simultaneously in the PL (Fig. 4A-C) and vice versa (Fig. 4D-F). Across the entire frequency spectrum, significantly more neurons were phase locked on correct trials (Table 1) ($\chi^2 = 4.27$, $P = 0.068$ for ACC spikes locked to PL LFP and $\chi^2 = 6.31$, $P = 0.029$ for PL spikes locked to ACC LFP).

Four ACC neurons phase locked to PL beta LFP exclusively on correct trials (Fig. 4A). On incorrect trials, there were no phase

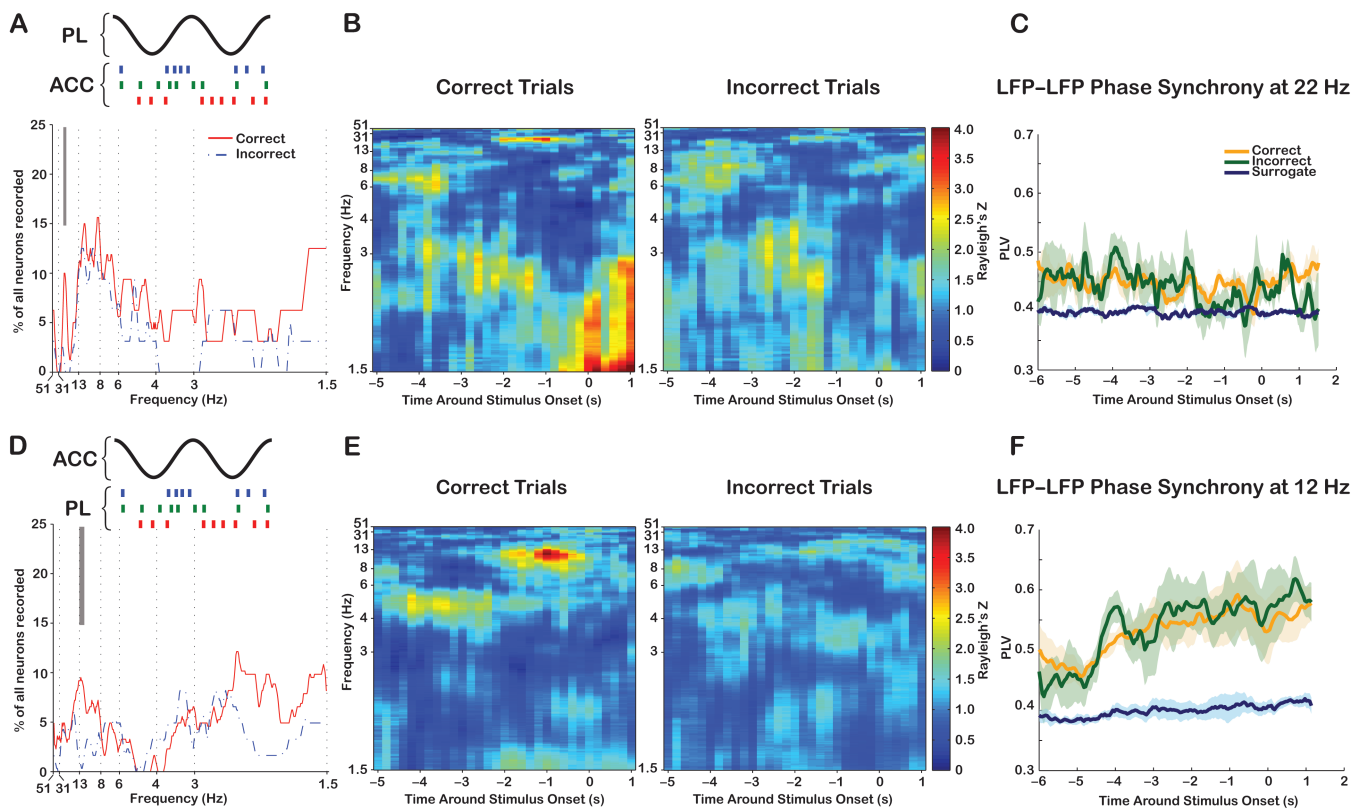


Figure 4. Between-region phase locking during the prestimulus period. (A) A schematic illustrating that the top panel (A–C) uses ACC neuron spikes and PL LFP oscillations. The proportion of neurons, between 1.5 and 50.0 Hz, that significantly phase lock to LFP from -2 to 0 s before stimulus onset on correct (red, solid) and incorrect (blue, dotted) trials. The width of the vertical bar indicates frequencies at which there was a reduction in the proportion of phase locked neurons on incorrect trials (χ^2 -squared test, $P < 0.05$). (B) Mean time-resolved phase locking strength (Rayleigh's Z) is averaged across the ACC neurons that phase locked to PL beta (13–30 Hz) LFP oscillations before stimulus onset. Stimulus is at $t = 0$ s. Rayleigh's Z was calculated in 2-s windows that were slid in 200-ms steps. Beta phase locking was present on correct trials and was not present on incorrect trials. The Between-region spike-field phase locking was centered at 22 Hz. (C) Prestimulus phase synchrony between the LFP signals recorded in the ACC and PL at 22 Hz. LFP-LFP phase synchrony was quantified over time using a within trial PLV. Stimulus onset is at $t = 0$ s. The mean PLV and its standard error (across rats) are shown for correct trials (orange), incorrect trials (green), and trial shuffled surrogate data (blue). During both correct and incorrect trials, a significantly high (compared with surrogate) level of LFP-LFP phase synchrony exists at 22 Hz before stimulus onset. (D–F) Same as above. (D) A schematic illustrating that the bottom panel uses PL neuron spikes and ACC LFP oscillations. A larger proportion of neurons phase locked to alpha oscillations on correct trials. (E) These PL neurons phase locked to ACC alpha (8–12 Hz) oscillations on correct trials, rather than incorrect trials, during the prestimulus period. The Between-region phase locking was centered at 12 Hz. (F) Prestimulus LFP-LFP phase synchrony at 12 Hz increases over time on correct (orange) and incorrect (green) trials. In both trial types, a significantly high level of LFP-LFP synchrony occurs at 12 Hz before stimulus onset.

locked neurons. The reduced proportion of phase locked neurons was centered at 22 Hz. Time-resolved phase locking strength (Fig. 4B) was reduced on incorrect trials (ANOVA; interaction: $F_{30,90} = 3.67$, $P < 0.001$). The difference between trial types occurred during the 2-s window prior to the stimulus onset (post hoc t -test, $t_0 = 4.37$, $P = 0.005$) and the window spanning -1.8 to 0.2 s around stimulus onset (post hoc t -test, $t_0 = 4.12$, $P = 0.006$). The phase locking observed during correct trials was greater than the level of synchrony expected by chance (ANOVA; main effect of trial: $F_{1,3} = 11.45$, $P = 0.043$; main effect of time: $F_{30,90} = 4.43$, $P < 0.0001$; interaction: $F_{30,90} = 5.73$, $P < 0.0001$). Again, these neurons exhibited no change in firing rate over time, and firing rate did not differ between trial types (ANOVA; interaction: $F_{39,117} = 0.637$, $P = 0.946$). In addition to spike-LFP phase synchrony, we also measured LFP-LFP phase synchrony at 22 Hz as further evidence that the ACC and PL were communicating in the beta frequency range. PLV at 22 Hz was not different between correct and incorrect trials (Fig. 4C); however, they both were significantly greater than the magnitude of synchrony expected by chance (ANOVA; interaction: $F_{654,1962} = 0.90$, $P = 0.95$).

Seven PL neurons were phase locked to ACC alpha LFP oscillations on correct trials, whereas none were phase locked on

incorrect trials (Fig. 4D). The reduction in the proportion of phase locked neurons was centered at 12 Hz. Time-resolved phase locking strength was larger on correct trials (Fig. 4E) (ANOVA; interaction: $F_{30,180} = 2.99$, $P < 0.001$). The difference between trial types occurred during 3 consecutive windows (ranging from -2 s to 0.4 s) around stimulus onset (post hoc t -tests for each time window; $t_{12} = 4.50$, $P < 0.001$; $t_{12} = 4.06$, $P = 0.002$; $t_{12} = 2.26$, $P = 0.043$). The phase locking strength on correct trials was not spurious (ANOVA; interaction: $F_{30,180} = 3.01$, $P < 0.0001$). These neurons exhibited no change in firing rate over time and firing rate did not differ between trial types (ANOVA; interaction: $F_{39,234} = 0.819$, $P = 0.770$). The LFP-LFP phase synchrony between brain regions at 12 Hz increased over time before stimulus onset (Fig. 4F). The PLV was not different between correct and incorrect trials but was higher than expected by chance (ANOVA; interaction: $F_{340,1020} = 1.02$, $P = 0.406$).

ACC Neurons Phase Locked to PL Beta Oscillations before the Stimulus and Then to PL Delta Oscillations after the Stimulus

As shown above, the ACC neurons that exhibited prestimulus phase locking to PL beta oscillations exclusively on correct

trials also phase locked to delta oscillations after stimulus onset (Fig. 4B). The average response latency (time of nose poke minus time of stimulus onset) on correct trials was 0.74 ± 0.20 s across all rats. This may indicate that neurons' delta phase locking on correct trials was due to changes in neural activity after stimulus onset and before the instrumental response to the chosen stimulus location. If this was the case, it is possible that these neurons also phase locked to delta oscillations on incorrect trials, but that it was not apparent in these plots because the average response latency on incorrect trials was 1.62 ± 0.20 s. Therefore, we characterized how this population of prestimulus beta phase locked neurons represented motor-related planning and/or motor execution after the stimulus onset.

Neural activity was aligned to the instrumental nose poke action and spike-LFP phase locking was measured before nose poke onset. Preparatory phase locking to PL delta oscillations occurred on both correct and incorrect trials and began less than 1 s before nose poke onset (Fig. 5A). The phase locking was of similar strength in both trial types; however, it began significantly earlier on correct trials (ANOVA using the mean from 1.5 to 2.4 Hz; main effect of trial: $F_{1,3} = 1.89$, $P = 0.263$;

main effect of time: $F_{25,75} = 1.96$, $P = 0.013$; interaction: $F_{25,75} = 0.75$, $P = 0.781$). Furthermore, the observed phase locking was not spurious (ANOVA; interaction: $F_{25,75} = 1.72$, $P = 0.0376$). Although trial shuffling reduced the average Rayleigh's Z (from -1 to 0 s before nose poke action) to 1.60, which is below a Z -score indicating 2 standard deviations from the mean, relatively high levels of chance synchrony were found with delta oscillations. There was no change in firing rate before nose poke onset. The phase locking of ACC spikes to PL delta oscillations was accompanied by an increase in PL delta band power that was not significantly different between trial types (Fig. 5B).

Discussion

Spike-LFP Phase Synchrony within and between the ACC and PL Occurs During Top-Down Attention

We investigated synchrony between and within the rat ACC and PL before the onset of a behaviorally relevant stimulus. Our analysis was focused primarily on the prestimulus period, which is when a preparatory top-down attention signal is

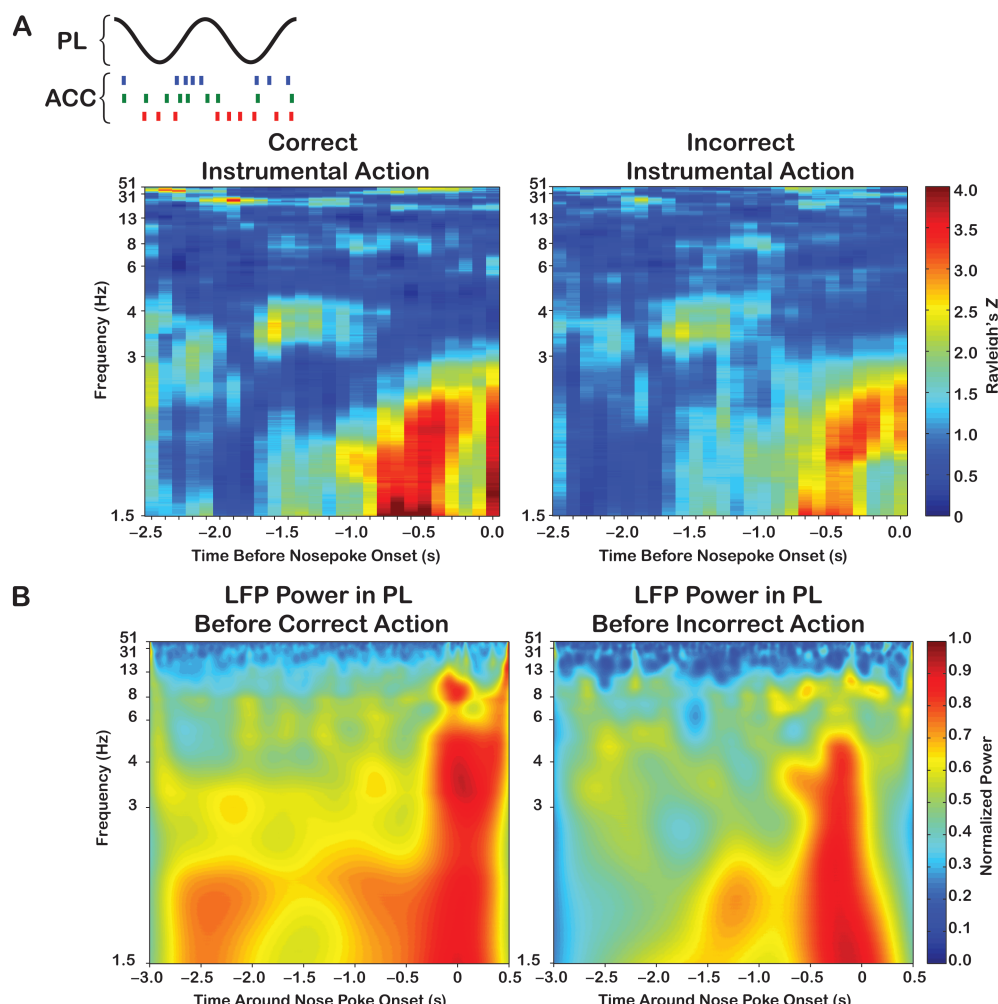


Figure 5. (A) A schematic illustrating that the top panel uses spikes from ACC neurons that were phase locked to PL beta oscillations during the prestimulus period. Neural activity is aligned to the onset of instrumental action (nose poke) at $t = 0$ s. The mean time-resolved phase locking strength was calculated across these neurons using a 1-s window, slid in 100-ms steps. Between-region delta oscillation phase locking occurs before the action during both correct and incorrect trials. (B) During the same time period, PL delta power is increased.

generated by the PFC (Chelazzi et al. 1993; Summerfield et al. 2006; Egner et al. 2008; Stokes et al. 2009; Sylvester et al. 2009; Totah et al. 2009; Noudoost et al. 2010) and exerts its effects upon sensory cortex neurons (Chelazzi et al. 1993; Luck et al. 1997; Roelfsema et al. 1997; Engel et al. 2001; Fries et al. 2001, 2008). We found that, at certain frequencies, within- and Between-region spike-LFP phase locking was reduced on incorrect trials, both in terms of the proportion of phase locked neurons and the strength of phase locking over time.

Within-region spike-LFP phase locked neurons shared a similar phase angle distribution. Given that Within-region synchrony aligns multiple spike trains in time as a mechanism for increasing overall postsynaptic output (Fries 2005, 2009), our data suggest that a population of neurons spike together in a temporal pattern aligned to the dynamics of local LFP oscillations and thus increase their output to downstream targets during top-down attention. These targets could include cortical areas involved in perception of the upcoming behaviorally relevant stimulus. Additionally, spike-LFP phase locking at the beta frequency was shared between both PL and ACC neurons that were phase locked to PL oscillations. Overall, these data support the hypothesis that neurons in the ACC drive beta LFP oscillations within the PL and entrain the local PL neurons to the beta rhythm. Future studies recording larger populations of neurons within a single subject simultaneously will be necessary to further test this hypothesis.

Another key finding of this study was that spike-LFP phase synchrony occurred across a wide range of frequencies, although at many frequencies the proportion of phase locked neurons was not different between correct and error trials. Direct corticocortical projections between the recorded locations in the ACC and contralateral PL exist in the rat (Jones et al. 2005) and could directly mediate this synchrony. The observation that synchrony occurred at many frequencies is consistent with the results of others (Canolty et al. 2010) and supports the hypothesis that oscillation phase synchrony could be used to form multiple neuronal assemblies and bind the relevant neurons together at relevant times (Siegel et al. 2009; Singer 2009). However, given that synchrony at only certain frequencies was predictive of behavioral performance, many of these other synchronous interactions may relate to other PFC dependent processing that occurs at the same time as preparatory attention.

On the other hand, we found that Between-region synchrony in the alpha and beta frequency ranges was related to behavioral performance, which suggests a role in the generation of a top-down attention signal. Beta frequency oscillations are associated with top-down attention (Roelfsema et al. 1997; Liang et al. 2002; Gross et al. 2006; Buschman and Miller 2007; Engel and Fries 2010). The degree of beta frequency coherence between frontal and parietal cortices during attention varies as a function of stimulus expectancy (Gross et al. 2006). Furthermore, beta frequency coherence between PFC areas and the lateral intraparietal area is increased during top-down attention, rather than bottom-up attention (Buschman and Miller 2007). The finding of increased alpha spike-LFP phase synchrony during top-down attention may seem paradoxical given that the alpha rhythm has been associated with a relaxed eyes closed state, or “idling,” and cognitive disengagement (Pfurtscheller 2001). However, other behaving animal electrophysiology studies, in addition to our study, have described increased alpha frequency LFP-LFP coherence between multiple visual cortex areas in the cat and increased Within-region

spike-LFP coherence in the alpha frequency in visual cortex during top-down attention (von Stein et al. 2000; Fries et al. 2008). Human EEG recordings also have demonstrated increased alpha phase synchrony between the PFC and visual cortex during attention (Palva S and Palva JM 2007; Zanto and Gazzaley 2009). Furthermore, it has been demonstrated that perturbing the PFC by transcranial magnetic stimulation reduces cross-cortical alpha synchrony, thus enhancing distracter-related visual cortex potentials and impairing attention task performance (Zanto and Gazzaley 2009). Thus, although the alpha rhythm has been associated with idling, our data and those of others indicate alpha rhythms may be used to suppress the neural representation of distracters (Klimesch et al. 2007). Notably, individuals with schizophrenia and ADHD exhibit increased distractibility and reduced alpha phase synchrony (Bob et al. 2008), which suggests that a reduction in cortical alpha synchrony could move inhibitory executive functions into a dysfunctional state.

In addition to Between-region spike-LFP phase synchrony during the prestimulus period, our study demonstrates that significant levels of Between-region LFP-LFP phase synchrony occur during the prestimulus period. According to the “communication through coherence” hypothesis, LFP-LFP phase synchrony is a mechanism for phase locked neuronal spikes to be communicated to their postsynaptic targets (Fries 2005). Although we did not find a difference in LFP-LFP phase synchrony between correct and incorrect trials, it is possible that LFP signals in 2 distant cortical regions synchronize and local mechanisms then govern whether or not local neurons will entrain to a distal rhythm.

The Same Neurons May Participate in Separate Neural Assemblies Supporting Attention and Action

We found that neurons in the ACC, which were phase locked to PL beta oscillations before stimulus onset, switched to delta oscillation phase locking after the stimulus and in preparation for the instrumental action. Previous work has shown that, in anticipation of an instrumental action in a rodent operant task, delta power increases within the rat PFC, and LFP-LFP delta frequency coherence increases between the PL and the nucleus accumbens core (Gruber et al. 2009). We replicated these findings and further demonstrated that Between-region spike-LFP delta synchrony occurs between the ACC and PL before an instrumental action and that these same ACC neurons participate in top-down attention. Beta oscillation phase locking before the stimulus was specific to correct trials, whereas the delta oscillation phase locking occurred during both correct and incorrect trials. Therefore, while coordination of neural activity between the ACC and PL may be necessary during top-down attention, coordination also may be needed for action planning and/or execution, regardless of whether or not the action is the correct decision. From a systems perspective, the shift from beta to delta frequency may indicate that the same population of neurons participates in multiple cognitive processes by joining different neuronal assemblies, at different times and at the service of different cognitive functions (Canolty et al. 2010).

Conclusion

These data demonstrate that areas of the PFC dynamically interact during attention and action. Phase synchrony of LFP

oscillations may serve as a neurophysiological mechanism by which multiple PFC areas can interact. These neurophysiological changes, which occur before the onset of a sensory stimulus, may serve to prime the neural representation of stimuli within sensory cortex and to improve the accuracy and speed of decision making and stimulus-guided action.

The fact that prestimulus phase synchrony was reduced during error trials suggests that diminished communication between multiple PFC areas could reflect an impaired cognitive state. Reduced synchrony between cortical regions has been observed in the brains of individuals with top-down attention deficits, such as those with ADHD and schizophrenia (Phillips and Silverstein 2003; Murias et al. 2007; Bob et al. 2008; Wang et al. 2009; Cubillo et al. 2010; Konrad and Eickhoff 2010; Mazaheri et al. 2010). Therefore, electrophysiological recordings, combined with pharmacological or genetic manipulations during the rodent preparatory attention task (Totah et al. 2009), may provide a useful paradigm for studying normal and impaired top-down attention.

Funding

US National Institute of Health—NIMH (grant numbers R01 MH084906 and R37 MH48404 to B.M.); Andrew Mellon Predoctoral Fellowship (to N.T.).

Notes

We are grateful to the Center for the Neural Basis of Cognition for the use of a computer cluster for data analysis. We thank Dr Guillaume Dumas (Centre de Recherche de l'Institut Cerveau-Moëlle) for assistance with MATLAB scripts for PLV analysis. *Conflict of Interest:* None declared.

References

- Berens P. 2009. CircStat: a MATLAB toolbox for circular statistics. *J Stat Software*. 31:1–21.
- Bob P, Palus M, Susta M, Glaslova K. 2008. EEG phase synchronization in patients with paranoid schizophrenia. *Neurosci Lett*. 447:73–77.
- Bressler SL, Tang W, Sylvester CM, Shulman GL, Corbetta M. 2008. Top-down control of human visual cortex by frontal and parietal cortex in anticipatory visual spatial attention. *J Neurosci*. 28:10056–10061.
- Buschman TJ, Miller EK. 2007. Top-down versus bottom-up control of attention in the prefrontal and posterior parietal cortices. *Science*. 315:1860–1862.
- Buzsáki G, Draguhn A. 2004. Neuronal oscillations in cortical networks. *Science*. 304:1926–1929.
- Canolty RT, Ganguly K, Kennerley SW, Cadieu CF, Koepsell K, Wallis JD, Carmena JM. 2010. Oscillatory phase coupling coordinates anatomically dispersed functional cell assemblies. *Proc Natl Acad Sci U S A*. 107:17356–17361.
- Chawla D, Lumer ED, Friston KJ. 2000. Relating macroscopic measures of brain activity to fast, dynamic neuronal interactions. *Neural Comput*. 12:2805–2821.
- Chawla D, Rees G, Friston KJ. 1999. The physiological basis of attentional modulation in extrastriate visual areas. *Nat Neurosci*. 2:671–676.
- Chelazzi L, Miller EK, Duncan J, Desimone R. 1993. A neural basis for visual search in inferior temporal cortex. *Nature*. 363:345–347.
- Chudasama Y, Passetti F, Rhodes SEV, Lopian D, Desai A, Robbins TW. 2003. Dissociable aspects of performance on the 5-choice serial reaction time task following lesions of the dorsal anterior cingulate, infralimbic and orbitofrontal cortex in the rat: differential effects on selectivity, impulsivity and compulsivity. *Behav Brain Res*. 146:105–119.
- Cubillo A, Halari R, Ecker C, Giampietro V, Taylor E, Rubia K. 2010. Reduced activation and inter-regional functional connectivity of fronto-striatal networks in adults with childhood Attention-Deficit Hyperactivity Disorder (ADHD) and persisting symptoms during tasks of motor inhibition and cognitive switching. *J Psychiatr Res*. 44:629–639.
- Desimone R, Duncan J. 1995. Neural mechanisms of selective visual attention. *Annu Rev Neurosci*. 18:193–222.
- Driver J, Frith CD. 2000. Shifting baselines in attention research. *Nat Rev Neurosci*. 1:147–148.
- Duncan J. 2001. An adaptive coding model of neural function in prefrontal cortex. *Nat Rev Neurosci*. 2:820–829.
- Egner T, Monti JMP, Tritschuh EH, Wieneke CA, Hirsch J, Mesulam MM. 2008. Neural integration of top-down spatial and feature-based information in visual search. *J Neurosci*. 28:6141–6151.
- Engel AK, Fries P. 2010. Beta-band oscillations—signalling the status quo? *Curr Opin Neurobiol*. 20:156–165.
- Engel AK, Fries P, Singer W. 2001. Dynamic predictions: oscillations and synchrony in top-down processing. *Nat Rev Neurosci*. 2:704–716.
- Fisher N. 1996. Statistical analysis of circular data. Cambridge (UK): Cambridge University Press.
- Fries P. 2005. A mechanism for cognitive dynamics: neuronal communication through neuronal coherence. *Trends Cogn Sci*. 9:474–480.
- Fries P. 2009. Neuronal gamma-band synchronization as a fundamental process in cortical computation. *Annu Rev Neurosci*. 32:209–224.
- Fries P, Reynolds JH, Rorie AE, Desimone R. 2001. Modulation of oscillatory neuronal synchronization by selective visual attention. *Science*. 291:1560–1563.
- Fries P, Womelsdorf T, Oostenveld R, Desimone R. 2008. The effects of visual stimulation and selective visual attention on rhythmic neuronal synchronization in macaque area V4. *J Neurosci*. 28:4823–4835.
- Fuster JM. 1995. Temporal processing. *Ann N Y Acad Sci*. 769:173–181.
- Fuster JM. 2001. The prefrontal cortex—an update: time is of the essence. *Neuron*. 30:319–333.
- Ghose GM, Maunsell JHR. 2002. Attentional modulation in visual cortex depends on task timing. *Nature*. 419:616–620.
- Gregoriou GG, Gotts SJ, Zhou H, Desimone R. 2009. High-frequency, long-range coupling between prefrontal and visual cortex during attention. *Science*. 324:1207–1210.
- Gross J, Schmitz F, Schnitzler I, Kessler K, Shapiro K, Hommel B, Schnitzler A. 2006. Anticipatory control of long-range phase synchronization. *Eur J Neurosci*. 24:2057–2060.
- Gruber AJ, Hussain RJ, O'Donnell P. 2009. The nucleus accumbens: a switchboard for goal-directed behaviors. *PLoS One*. 4:e5062.
- Hussar CR, Pasternak T. 2009. Flexibility of sensory representations in prefrontal cortex depends on cell type. *Neuron*. 64:730–743.
- Johnston K, Levin HM, Koval MJ, Everling S. 2007. Top-down control-signal dynamics in anterior cingulate and prefrontal cortex neurons following task switching. *Neuron*. 53:453–462.
- Jones BF, Groenewegen HJ, Witter MP. 2005. Intrinsic connections of the cingulate cortex in the rat suggest the existence of multiple functionally segregated networks. *Neuroscience*. 133:193–207.
- Kastner S, Pinsk MA, De Weerd P, Desimone R, Ungerleider LG. 1999. Increased activity in human visual cortex during directed attention in the absence of visual stimulation. *Neuron*. 22:751–761.
- Klimesch W, Sauseng P, Hanslmayr S. 2007. EEG alpha oscillations: the inhibition-timing hypothesis. *Brain Res Rev*. 53:63–88.
- Konrad K, Eickhoff SB. 2010. Is the ADHD brain wired differently? A review on structural and functional connectivity in attention deficit hyperactivity disorder. *Hum Brain Mapp*. 31:904–916.
- LaBerge D. 2002. Attentional control: brief and prolonged. *Psychol Res*. 66:220–233.
- Lachaux JP, Rodriguez E, Martinerie J, Varela FJ. 1999. Measuring phase synchrony in brain signals. *Hum Brain Mapp*. 8:194–208.
- Le Van Quyen M, Bragin A. 2007. Analysis of dynamic brain oscillations: methodological advances. *Trends Neurosci*. 30:365–373.
- Liang H, Bressler SL, Ding M, Truccolo WA, Nakamura R. 2002. Synchronized activity in prefrontal cortex during anticipation of visuomotor processing. *Neuroreport*. 13:2011–2015.
- Linkenkaer-Hansen K, Nikouline VV, Palva JM, Ilmoniemi RJ. 2001. Long-range temporal correlations and scaling behavior in human brain oscillations. *J Neurosci*. 21:1370–1377.

- Linkenkaer-Hansen K, Nikulin VV, Palva S, Ilmoniemi RJ, Palva JM. 2004. Prestimulus oscillations enhance psychophysical performance in humans. *J Neurosci.* 24:10186–10190.
- Luck SJ, Chelazzi L, Hillyard SA, Desimone R. 1997. Neural mechanisms of spatial selective attention in areas V1, V2, and V4 of macaque visual cortex. *J Neurophysiol.* 77:24–42.
- Mazaheri A, Coffey-Corina S, Mangun GR, Bekker EM, Berry AS, Corbett BA. 2010. Functional disconnection of frontal cortex and visual cortex in attention-deficit/hyperactivity disorder. *Biol Psychiatry.* 67:617–623.
- Miller EK, Cohen JD. 2001. An integrative theory of prefrontal cortex function. *Annu Rev Neurosci.* 24:167–202.
- Moghaddam B, Homayoun H. 2007. Divergent plasticity of prefrontal cortex networks. *Neuropsychopharmacology.* 33:42–55.
- Murias M, Swanson JM, Srinivasan R. 2007. Functional connectivity of frontal cortex in healthy and ADHD children reflected in EEG coherence. *Cereb Cortex.* 17:1788–1799.
- Narayanan NS, Laubach M. 2006. Top-down control of motor cortex ensembles by dorsomedial prefrontal cortex. *Neuron.* 52:921–931.
- Narayanan NS, Laubach M. 2009. Delay activity in rodent frontal cortex during a simple reaction time task. *J Neurophysiol.* 101:2859–2871.
- Ng C-W, Noblejas MI, Rodefer JS, Smith CB, Poremba A. 2007. Double dissociation of attentional resources: prefrontal versus cingulate cortices. *J Neurosci.* 27:12123–12131.
- Niki H, Watanabe M. 1979. Prefrontal and cingulate unit activity during timing behavior in the monkey. *Brain Res.* 171:213–224.
- Noudoost B, Chang MH, Steinmetz NA, Moore T. 2010. Top-down control of visual attention. *Curr Opin Neurobiol.* 20:183–190.
- Orr JM, Weissman DH. 2009. Anterior cingulate cortex makes 2 contributions to minimizing distraction. *Cereb Cortex.* 19:703–711.
- Palva S, Palva JM. 2007. New vistas for alpha-frequency band oscillations. *Trends Neurosci.* 30:150–158.
- Passetti F, Chudasama Y, Robbins TW. 2002. The frontal cortex of the rat and visual attentional performance: dissociable functions of distinct medial prefrontal subregions. *Cereb Cortex.* 12:1254–1268.
- Peters YM, O'Donnell P, Carelli RM. 2005. Prefrontal cortical cell firing during maintenance, extinction, and reinstatement of goal-directed behavior for natural reward. *Synapse.* 56:74–83.
- Pfurtscheller G. 2001. Functional brain imaging based on ERD/ERS. *Vision Res.* 41:1257–1260.
- Phillips WA, Silverstein SM. 2003. Convergence of biological and psychological perspectives on cognitive coordination in schizophrenia. *Behav Brain Sci.* 26:65–82; discussion 82–137.
- Posner MI, Petersen SE. 1990. The attention system of the human brain. *Annu Rev Neurosci.* 13:25–42.
- Pragay EB, Mirsky AF, Nakamura RK. 1987. Attention-related unit activity in the frontal association cortex during a go/no-go visual discrimination task. *Exp Neurol.* 96:481–500.
- Rainer G, Rao SC, Miller EK. 1999. Prospective coding for objects in primate prefrontal cortex. *J Neurosci.* 19:5493–5505.
- Rodriguez E, George N, Lachaux JP, Martinerie J, Renault B, Varela FJ. 1999. Perception's shadow: long-distance synchronization of human brain activity. *Nature.* 397:430–433.
- Roelfsema PR, Engel AK, König P, Singer W. 1997. Visuomotor integration is associated with zero time-lag synchronization among cortical areas. *Nature.* 385:157–161.
- Roelofs A, van Turennout M, Coles MGH. 2006. Anterior cingulate cortex activity can be independent of response conflict in Stroop-like tasks. *Proc Natl Acad Sci U S A.* 103:13884–13889.
- Siegel M, Warden MR, Miller EK. 2009. Phase-dependent neuronal coding of objects in short-term memory. *Proc Natl Acad Sci U S A.* 106:21341–21346.
- Singer W. 2009. Distributed processing and temporal codes in neuronal networks. *Cogn Neurodyn.* 3:189–196.
- Sirota A, Montgomery S, Fujisawa S, Isomura Y, Zugaro M, Buzsáki G. 2008. Entrainment of neocortical neurons and gamma oscillations by the hippocampal theta rhythm. *Neuron.* 60:683–697.
- Stokes M, Thompson R, Nobre AC, Duncan J. 2009. Shape-specific preparatory activity mediates attention to targets in human visual cortex. *Proc Natl Acad Sci U S A.* 106:19569–19574.
- Summerfield C, Egner T, Greene M, Koechlin E, Mangels J, Hirsch J. 2006. Predictive codes for forthcoming perception in the frontal cortex. *Science.* 314:1311–1314.
- Sylvester CM, Shulman GL, Jack AI, Corbetta M. 2009. Anticipatory and stimulus-evoked blood oxygenation level-dependent modulations related to spatial attention reflect a common additive signal. *J Neurosci.* 29:10671–10682.
- Totah NKB, Kim YB, Homayoun H, Moghaddam B. 2009. Anterior cingulate neurons represent errors and preparatory attention within the same behavioral sequence. *J Neurosci.* 29:6418–6426.
- Varela F, Lachaux JP, Rodriguez E, Martinerie J. 2001. The brainweb: phase synchronization and large-scale integration. *Nat Rev Neurosci.* 2:229–239.
- von Stein A, Chiang C, König P. 2000. Top-down processing mediated by interareal synchronization. *Proc Natl Acad Sci U S A.* 97:14748–14753.
- Wang L, Zhu C, He Y, Zang Y, Cao Q, Zhang H, Zhong Q, Wang Y. 2009. Altered small-world brain functional networks in children with attention-deficit/hyperactivity disorder. *Hum Brain Mapp.* 30:638–649.
- Womelsdorf T, Schoffelen J-M, Oostenveld R, Singer W, Desimone R, Engel AK, Fries P. 2007. Modulation of neuronal interactions through neuronal synchronization. *Science.* 316:1609–1612.
- Zanto TP, Gazzaley A. 2009. Neural suppression of irrelevant information underlies optimal working memory performance. *J Neurosci.* 29:3059–3066.